Journal of Magnetic Resonance 208 (2011) 156–162

Contents lists available at ScienceDirect

Journal of Magnetic Resonance

journal homepage: www.elsevier.com/locate/jmr

The heterogeneity of segmental dynamics of filled EPDM by ^{1}H transverse relaxation NMR

D. Moldovan [a], R. Fechete [a,*], D.E. Demco [a,b,*], E. Culea [a], B. Blümich [c], V. Herrmann [d], M. Heinz [e]

[a] Technical University of Cluj-Napoca, Daicoviciu 1, R-400020 Cluj-Napoca, Romania
[b] DWI an der RWTH-Aachen University e.V. Pauwelsstr. 8, D-52056 Aachen, Germany
[c] Institut für Technische und Makromolekulare Chemie, RWTH-Aachen University, Worringerweg 1, D-52056 Aachen, Germany
[d] Hochschule für Angewandte Wissenschaften, Fachhochschule Würzburg-Schweinfurt, Röntgenring 8, 97070 Würzburg, Germany
[e] Evonik Degussa GmbH, Harry-Kloepfer Str. 1, 50997 Köln, Germany

ARTICLE INFO

Article history:
Received 21 July 2010
Revised 29 October 2010
Available online 5 November 2010

Keywords:
Proton residual second moment
Correlation time
Distributions
EPDM
Carbon-black filled elastomers

ABSTRACT

Residual second moment of dipolar interactions $\tilde{M}_2$ and correlation time segmental dynamics distributions were measured by Hahn-echo decays in combination with inverse Laplace transform for a series of unfilled and filled EPDM samples as functions of carbon-black N683 filler content. The fillers–polymer chain interactions which dramatically restrict the mobility of bound rubber modify the dynamics of mobile chains. These changes depend on the filler content and can be evaluated from distributions of $\tilde{M}_2$. A dipolar filter was applied to eliminate the contribution of bound rubber. In the first approach the Hahn-echo decays were fitted with a theoretical relationship to obtain the average values of the ^{1}H residual second moment $\langle\tilde{M}_2\rangle$ and correlation time $\langle\tau_c\rangle$. For the mobile EPDM segments the power-law distribution of correlation function was compared to the exponential correlation function and found inadequate in the long-time regime. In the second approach a log-Gauss distribution for the correlation time was assumed. Furthermore, using an averaged value of the correlation time, the distributions of the residual second moment were determined using an inverse Laplace transform for the entire series of measured samples. The unfilled EPDM sample shows a bimodal distribution of residual second moments, which can be associated to the mobile polymer sub-chains ($\tilde{M}_2 \cong 6.1$ rad^2 s^{-2}) and the second one associated to the dangling chains $\tilde{M}_2 \cong 5.4$ rad^2 s^{-2}). By restraining the mobility of bound rubber, the carbon-black fillers induce diversity in the segmental dynamics like the apparition of a distinct mobile component and changes in the distribution of mobile and free-end polymer segments.

1. Introduction

Local diversity plays an essential role in the development of new materials with improved properties. In particular, the nanocomposite elastomers are important materials extensively used in the rubber industry. Due to their demanding applications, such materials must fulfill many requirements. Usually, these elastomers are characterized by high elasticity even at large deformation, high resistance to swelling in solvents, high resistance to corrosion, and long service life [1]. The presence of nano–filler particles in rubbery materials enhances the mechanical properties [1–4]. The main contribution is due to filler volume and surface effects, filler–filler and filler–polymer matrix interactions. The physical interactions of the rubber chains with the filler surface can provide quasi-permanent junctions in the rubber matrix, which are not removed even after extensive solvent extraction. Due to this chain adsorption in the direct vicinity of filler particles, the rubber chain mobility is physically constrained [1–9]. For polymer matrices with higher molecular weight, the greater filler reinforcement is due to filler particle association through chain adsorption and bridging [9]. Therefore the mobile polymer segment dynamics play an important role in the final product properties. The properties of mobile rubber are influenced by the filler–polymer interaction which depends on the filler type and filler content.

The distribution of the chain lengths between crosslink junctions of polymer networks was discussed in the past by Sandakov et al. [10]. The method is based on the relation between the high-temperature free-induction decay and the assumption of Gauss distribution for the residual dipolar couplings. Moreover, the molecular weight distribution function of the network was not generated by the inverse Laplace transform.

The heterogeneities of filler–filler interactions and polymer chain dynamics of filled and unfilled EPDM samples were recently discussed in Ref. [11]. Hereby the heterogeneous effects of reinforcing nano-particles were characterized by the Payne effect that

* Corresponding authors. Address: DWI an der RWTH-Aachen University e.V. Pauwelsstr. 8, D-52056 Aachen, Germany. Fax: +49 241 888 185 (D.E. Demco).
E-mail addresses: rfechete@phys.utcluj.ro (R. Fechete), demco@mc.rwth-aachen.de (D.E. Demco).

1090-7807/$ - see front matter © 2010 Elsevier Inc. All rights reserved.
doi:10.1016/j.jmr.2010.10.019

was observed as decay curves of the storage modulus as a function of the shear–strain amplitude. The full decay of these curves was analyzed by one-dimensional Laplace-like inversion to obtain the distribution of filler–filler interactions. These distributions reveal the existence of week, medium, and strong filler–filler interactions, which were associated to the direct and indirect matrix-mediated filler–filler interactions [11].

Various NMR methods have been implemented to describe the polymer segmental dynamics which are usually correlated with the elastomers macroscopic properties [7,8,11–30]. These are based on the measurement of ^{1}H and ^{13}C longitudinal (T_1), transverse (T_2) and longitudinal in rotating frame ($T_{1\rho}$) relaxation times [7,8,11–20], multiple-quantum NMR [21–25], cross-polarization and ^{1}H magnetization exchange [20], Hahn echo [7,12,27], solid-echo [17,28], and magic echo [29,30] decays were used to extract parameters that describe the segmental dynamics. The heterogeneity of the segmental dynamics was characterized for the filled EPDM samples by ^{1}H low-field NMR T_1, T_2, and $T_{1\rho}$ relaxation time distributions [11]. The second van Vleck moment M_2 and the correlation time τ_c are preferred parameters for describing the segmental dynamics [17,18,21,25–30]. Proton NMR Hahn-echo relaxation was used to study the adsorption of polymer chains to the surface of carbon-black fillers for EPDM/carbon black networks in cured and uncured conditions [7]. They showed that a continuous EPDM/carbon black physical network is formed in the bound rubber and polymer chain bridges are connect to the carbon-black aggregates. Along these polymer chains, the segmental dynamics can be characterized by correlation times, which are the times of reorientation of functional groups in the repeat units. Therefore, the bound rubber is characterized by correlation times, with several orders of magnitude higher than those of mobile segments.

The aim of this work is to study the polymer network dynamics for a series of EPDM rubber samples filled with N683 carbon black nano-particles of various contents from 20 phr to 70 phr. By applying a dipolar filter to the Hahn-echo pulse sequence, only the signal arising from mobile polymer segments is measured. Finally, the distributions of $\tilde{M}_2$ are used to describe the dynamics heterogeneities of polymer segments in filled EPDM samples.

2. Experimental

2.1. Samples

A series of EPDM samples with different carbon-black (N683) filler concentrations of 20, 40, 60 and 70 phr (parts of filler per hundred parts of polymer by weight) was prepared at Degusa (Evonik), Germany. The samples have been not cross-linked. We mixed the EPDM polymer (KELTAN 512) with the filler in an internal mixer and draw out a rubber sheet on a mill. The value of T_g of KELTAN 512 is in the range of −55 °C. For comparison, an unfilled reference EPDM sample was also tested in the same way as the filled samples. A summary of carbon-black N683 filler properties can be found in Table 1.

2.2. NMR experiments

The proton Hahn-echo decay was measured using an mq20 Bruker NMR time–domain spectrometer working at homogeneous magnetic fields with a proton frequency of 19.88 MHz. During all measurement the temperature of the permanent magnet and the sample was kept constant at 35 ± 0.1 °C. The Hahn-echo pulse sequence with a simple dipolar filter is presented in Fig. 1. The length of the 90_x tipping pulse was found between 4.6 and 5.4 μs depending on filler type and content. The 180_y refocusing pulse was set to the same amplitude and double the time as the tipping pulse. Since the longitudinal relaxation time T_1 for this series of samples was around 50 ms, recycle delays of 0.4 s assure full remagnetization for all samples [11]. A total of 256 scans were recorded in each measurement. The dashed vertical line in Fig. 1 marks the dipolar filter of duration τ_f = 200 μs which eliminates the signal contributions of bound rubber which are associated with a short transverse relaxation decay. This delay moves the fast decaying NMR signal from bound rubber out of the acquisition window. For all samples the echo time starts at 200 μs and was increased in 32 unequal steps up to 2 ms (Fig. 2). In order to be compared, all curves are normalized to the amplitude of the first measured point. Differences between the ^{1}H Hahn-echo decays for the N683 filled EPDM sample with different filler contents (from 20 phr to 70 phr) are shown in Fig. 2.

Table 1
The characteristics of N683 carbon-black filler. STSA represents the statistical thickness of the surface area, BET denotes the nitrogen adsorption methods, and CTAB is the cethyl-trimethyl-ammonium bromide adsorption method. The percolation threshold was measured by the electrical resistance method.

Filler type	Average particle size (nm)	Surface area (m^2/g)			Percolation threshold (phr)
		STSA	BET	CTAB	
N683	73	34	36	40	60–70

3. Results and discussion

3.1. Hahn-echo decay

The normalized Hahn-echo (HE) signal for a spin-½ pair can be written as [27,28]:

$$\frac{S_{HE}(2\tau)}{S_{HE}(0)} = \langle \cos(2\bar{\omega}_D\tau)\rangle \left\langle \exp\left[-2\sqrt{\frac{3}{2}}\tilde{M}_2\tau_c^2(e^{-\tau/\tau_c}-1+\tau/\tau_c)\right] \times \exp\left[-\sqrt{\frac{3}{2}}\tilde{M}_2\tau_c^2(1-2e^{-\tau/\tau_c}+e^{-2\tau/\tau_c})\right]\right\rangle, \quad (1)$$

where $\bar{\omega}_D$ is the residual dipolar. The symbol $\langle(\ldots)\rangle \equiv \langle\langle\rangle_{\vec{R}}\rangle_\beta$ represents the average over the statistical ensemble which includes

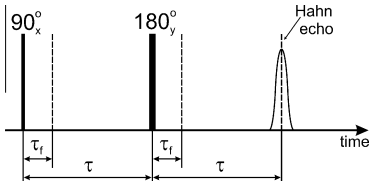

Fig. 1. The Hahn-echo pulse sequence with the dipolar filter which acts during the time interval shown by the vertical dashed line. It is used to measure the residual second moment $\tilde{M}_2$ and distribution of correlation time τ_c.

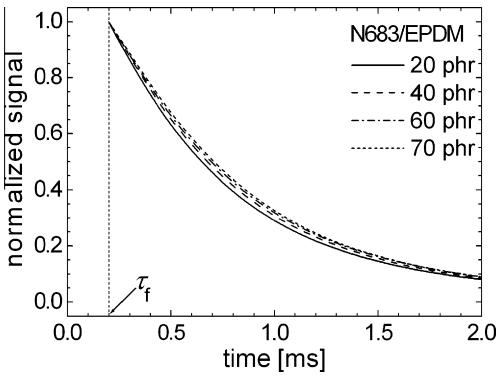

Fig. 2. Normalized Hahn-echo decays for the EPDM sample reinforced with the N683 filler as a function of the filler content from 20 phr to 70 phr. The vertical dashed line represents the duration of the dipolar filter.

two separate averages, one over the length of the reduced end-to-end vector $\vec{R}$, denoted by $\langle(\ldots)\rangle_{\vec{R}}$ and the other over the azimuthally angle β denoted by $\langle(\ldots)\rangle_{\beta}$ [29].

In the derivation of Eq. (1), the correlation function of the dipolar fluctuation, $C(t)$ is considered to be of the exponential form [15,17,28,29], i.e.,

$$C(t) = \langle \Delta\omega_D(t)\Delta\omega_D(0)\rangle = \langle \Delta\omega_D^2(0)\rangle \exp\{-t/\tau_c\} = \widetilde{M}_2 \exp\{-t/\tau_c\}, \quad (2)$$

where the residual dipolar coupling is denoted by $\widetilde{M}_2 \equiv \langle \Delta\omega_D^2(0)\rangle$, and τ_c is the correlation time of the segmental motions. Moreover, a second assumption made in Eq. (1) is that the Hahn-echo signal can be written as a product of averaged (av) and fluctuating (fl) contributions, i.e.,

$$\frac{S_{HE}(2\tau)}{S_{HE}(0)} = \langle S_{av}(\bar{\omega}_D,\tau)\rangle\langle S_{fl}(\widetilde{M}_2,\tau_c,\tau)\rangle, \quad (3)$$

where the average (or solid-like) contribution is given by,

$$S_{av}(\bar{\omega}_D,\tau) = \cos(2\bar{\omega}_D\tau), \quad (4)$$

and the fluctuating (or liquid-like) contribution is given by,

$$S_{fl}(\widetilde{M}_2,\tau_c,\tau) = \exp\left[-\sqrt{\frac{3}{2}}\widetilde{M}_2\tau_c^2\left(e^{-2\tau/\tau_c}+2\tau/\tau_c-1\right)\right]. \quad (5)$$

3.2. The contribution of the mobile polymer segments to the Hahn-echo decay

Three dynamic components of polymer chains in filled elastomers can be considered (Fig. 3). They are (i) the bound rubber, (ii) the interface between bound rubber and mobile chains, and (iii) the mobile chains, with one end connected via an interface to the bound rubber while the second end can be free or, as in the majority of cases, connected to another filler cluster. One can consider that the bound polymer chains are characterized by motions strongly restricted compared to these in the interface and of the mobile chain segments.

The full NMR signal can be written as a sum of signals arising from the bound (b) and mobile (m) contributions,

$$\frac{S_{HE}(2\tau)}{S_{HE}(0)} = \left\langle S_{av}^{b}(\bar{\omega}_D^{b},\tau)\right\rangle\left\langle S_{fl}\left(\widetilde{M}_2^{b},\tau_c^{b},\tau\right)\right\rangle + \left\langle S_{av}^{m}(\bar{\omega}_D^{m},\tau)\right\rangle\left\langle S_{fl}\left(\widetilde{M}_2^{m},\tau_c^{m},\tau\right)\right\rangle, \quad (6)$$

Since the motion of the bound rubber segments is restricted, the residual dipolar coupling constant is larger than the residual dipolar coupling constant of the mobile chain segments, $\bar{\omega}_D^{b} \gg \bar{\omega}_D^{m}$ and $\tau_c^{m} \ll \tau_c^{b}$.

The above arguments justify the assumption that, the NMR signal arising from the bound chain segments is filtered out and only the normalized Hahn-echo decay which arises from mobile chain segments is measured,

$$\frac{S_{HE}(2\tau)}{S_{HE}(0)} = \langle S_{av}^{m}(\bar{\omega}_D^{m},\tau)\rangle\left\langle S_{fl}(\widetilde{M}_2^{m},\tau_c^{m},\tau)\right\rangle. \quad (7)$$

In the presence of an efficient dipolar filter the final relationship that expresses the normalized Hahn-echo decay is given by,

$$\frac{S_{HE}(2\tau)}{S_{HE}(0)} = \left\langle S_{fl}\left(\widetilde{M}_2^{m},\tau_c^{m},\tau\right)\right\rangle = \left\langle \exp\left[-\sqrt{\frac{3}{2}}\widetilde{M}_2\tau_c^2\left(e^{-2\tau/\tau_c}+2\tau/\tau_c-1\right)\right]\right\rangle, \quad (8)$$

where $\widetilde{M}_2$ represents the residual second moment of the mobile chain segments and τ_c the associated correlation time.

3.3. Average ^{1}H residual second moment and correlation time approximation

The normalized Hahn-echo decay for the EPDM sample with 20 phr N683 filler, is presented in Fig. 4. We consider that the average over the statistical ensemble can be introduced in the exponential function in Eq. (8). This can be shown to be valid for small values of τ/τ_c. Then, we can write,

$$\frac{S_{HEc}(2\tau)}{S_{HEc}(0)} = \exp\left[-\sqrt{\frac{3}{2}}\langle\widetilde{M}_2\rangle\langle\tau_c\rangle^2\left(e^{-2\tau/\langle\tau_c\rangle}+2\tau/\langle\tau_c\rangle-1\right)\right], \quad (9)$$

where we have introduced the averaged residual second moment $\langle\widetilde{M}_2\rangle$ and the averaged value of correlation time $\langle\tau_c\rangle$. In order to evaluate the $\langle\widetilde{M}_2\rangle$ and $\langle\tau_c\rangle$ quantities, a program based on the Levenberg–Marquardt procedure was written in C++ that fits the

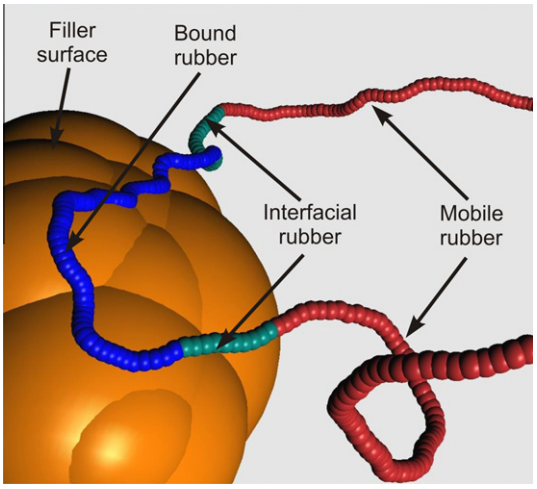

Fig. 3. Schematic drawing of polymer chains at the interface between the EPDM rubber chains and clustered nanofiller-particles. The chain dynamics of the bond rubber is restricted by the strong direct interaction of fillers particles and polymer segments. This interaction influences also the dynamics of the intermediate chain segments.

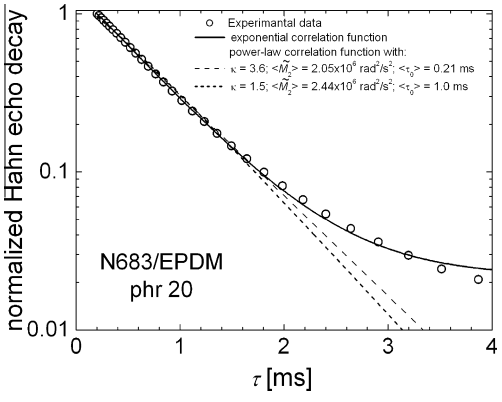

Fig. 4. Normalized Hahn-echo decay for the EPDM filled with 20 phr N683 (open circles). The continue line represents the best fit ($\chi^2 = 48.5\times10^{-5}$) using an exponential correlation function (Eq. (2)) with $\langle\widetilde{M}_2\rangle = 5.7\times10^6$ rad^2 s^{-2} and $\tau_c = 115$ μs. The dashed line represents the best fit ($\chi^2 = 137\times10^{-5}$) using the power-law correlation function to describe the Hahn-echo decay (Eq. (11)) with averaged values of the residual second moment $\widetilde{M}_2 = 2.1\times10^6$ rad^2 s^{-2}, $\tau_0 = 0.21$ ms, and $\kappa = 3.6$. The short dashed line represent the best fit ($\chi^2 = 175\times10^{-5}$) of the Hahn-echo decay using the power-law correlation function with a fixed value for $\kappa = 1.5$ and $\widetilde{M}_2 = 2.4\times10^6$ rad^2 s^{-2}, $\tau_0 = 1$ ms .

experimental data using Eq. (9). The best-fit curve characterized by the averages $\langle \widetilde{M}_2 \rangle = 5.7 \times 10^6$ rad^2 s^{-2} and $\langle \tau_c \rangle = 115.1$ μs is presented in Fig. 4 (continue line) for the 20 phr N683 sample. The initial time regime is well approximated but a small deviation from experimental data is observed at larger echo time values.

The best fit parameters $\langle \widetilde{M}_2 \rangle$ and $\langle \tau_c \rangle$ for the unfilled and N689 filled EPDM samples with 20 phr up to 70 phr filler content are presented in Table 2.

3.4. The power-law correlation function

Often, the polymer chain dynamics is described by power-law correlation functions [16,31]. Kimmich and coworkers [16] have used such power-law function to fit a dipolar correlation quotients for the *short* component of the stimulated and primary echoes measured for cross-linked SBR samples. In the following we will investigate if the power-law correlation function is suitable to describe the dynamics of mobile EPDM segments in carbon-black filled samples for the Hahn-echo decay in the time domain investigated. For that we will consider the power-law correlation function discussed in Ref. [16],

$$C(t) = \begin{cases} \widetilde{M}_2 & \text{for } |t| < \tau_0 \\ \widetilde{M}_2 \left(\frac{\tau_0}{|t|}\right)^{\kappa} & \text{for } |t| \geqslant \tau_0 \end{cases}, \tag{10}$$

where the time constant τ_0 describes the onset of the decay.

Using the above correlation function the decay of the Hahn echoes function of echo time is given by,

$$\frac{S_{\mathrm{HEc}}(2\tau)}{S_{\mathrm{HEc}}(0)} \propto \begin{cases} \exp\left\{-\sqrt{\frac{3}{2}}\langle \widetilde{M}_2 \rangle \left[2\tau \cdot \langle \tau_0 \rangle - \frac{\langle \tau_0 \rangle^2}{2}\right]\right\} \\ \text{for } 2\tau < \langle \tau_0 \rangle \\ \exp\left\{-\sqrt{\frac{3}{2}}\langle \widetilde{M}_2 \rangle \left[2\tau \cdot \langle \tau_0 \rangle - \frac{\langle \tau_0 \rangle^2}{2} + \frac{2\tau \cdot \langle \tau_0 \rangle \left(2^{1-\kappa}\tau^{1-\kappa}\langle \tau_0 \rangle^{\kappa-1} + \kappa - 2\right) + \langle \tau_0 \rangle^2 (1-\kappa)}{(2-\kappa)(1-\kappa)}\right]\right\} \\ \text{for } 2\tau \geqslant \langle \tau_0 \rangle \end{cases}, \tag{11}$$

where $\kappa \neq 1, 2$.

The best fit using Eq. (11) of the Hahn-echo decay for the mobile EPDM chains filled with N683 carbon black nano-particles is shown in Fig. 4 with dashed line. The value of residual second moment $\langle \widetilde{M}_2 \rangle = 2.05 \times 10^6$ rad^2 s^{-2} obtained from fit is approximately 2–3 times smallest then the value obtained from the fit of the same experimental data with Eq. (9). Nevertheless, compared to the best fit using the exponential correlation function, characterized by a reduced value for the merit function $\chi^2 = 48.5 \times 10^{-5}$ (continuous line in Fig. 4), the approximation of the experimental data using the power-law distribution function can describe only the initial decay and deviate substantially from these data at longer echo times. Therefore, the merit function for the full decay is larger ($\chi^2 = 137 \times 10^{-5}$) then, in the case of the exponential correlation function. Moreover, the value of power-law exponent $\kappa = 3.6$ was found larger than those reported in Refs. [16,31]. Another test was performed for $\kappa = 1.5$ and $\langle \tau_0 \rangle = 1$ *ms* fixed parameters as given in Ref. [16] and shown in Fig. 4 with short dashed line. In this case the residual second moment of $\langle \widetilde{M}_2 \rangle = 2.4 \times 10^6$ rad^2 s^{-2} was obtained and the merits function is $\chi^2 = 175 \times 10^{-5}$. This quantity is even larger than before and the deviation form experimental data is observed earlier. In conclusion, it is clear that the exponential correlation function describes more realistic the segmental dynamics of filled EPDM samples in the investigated time regime.

3.5. Distribution of the correlation time

The local dynamics and structural heterogeneity in filled networks suggest to consider distributions of the ^{1}H residual second moments $\widetilde{M}_2$ and/or correlation times τ_c. Such data analysis involves Laplace inversion of the measured Hahn-echo decay as a function of the echo time in order to extract the residual second moment and/or correlation time distributions. We consider in the following the average over parameter distributions in the equation of the Hahn-echo decay function. This could be represented as an integral over the exponential function weighted by the distribution function $f(\widetilde{M}_2, \tau_c)$, i.e.,

$$\frac{S_{\mathrm{HEc}}(2\tau)}{S_{\mathrm{HEc}}(0)} = \int_0^\infty \int_0^\infty f\left(\widetilde{M}_2, \tau_c\right) \times \exp\left[-\sqrt{\frac{3}{2}}\widetilde{M}_2 \tau_c^2 \left(\mathrm{e}^{-2\tau/\tau_c} + 2\tau/\tau_c - 1\right)\right] d\widetilde{M}_2 d\tau_c. \tag{12}$$

The distribution function $f(\widetilde{M}_2, \tau_c)$ can be obtained from Eq. (12) by inverse Laplace-like transformation [32–34]. The inverse Laplace transformation is an ill-conditioned problem that requires special care. A small change in the input data may lead to large changes in the result. This problem was nicely addressed by implementing a regularisation procedure in a fast inversion algorithm [34].

As the normalized Hahn-echo decays are measured in one–dimension we cannot perform a transformation to receive a two–dimensional distribution function of $\widetilde{M}_2$ and τ_c. Therefore, in the following, we consider only the distributions of the correlation time τ_c for the averaged values of residual second moment $\langle \widetilde{M}_2 \rangle$ obtained in the previous section, i.e.,

$$\frac{S_{\mathrm{HEc}}(2\tau)}{S_{\mathrm{HEc}}(0)} = \int_0^\infty f(\tau_c) \exp\left[-\sqrt{\frac{3}{2}}\langle \widetilde{M}_2 \rangle \tau_c^2 \left(e^{-2\tau/\tau_c} + 2\tau/\tau_c - 1\right)\right] d\tau_c. \tag{13}$$

The normalized distribution of the correlation time τ_c for the EPDM sample with 70 phr N683 filler obtained by one-dimensional Laplace inversion using Eq. (13) with an average value of the residual second moment of $\langle \widetilde{M}_2 \rangle = 1.76 \times 10^6$ rad^2 s^{-2} is shown in Fig. 5a. A main peak centered at a ~360 μs appears but also a small peak is observed at lower correlation time. This could be an indication of the existence of fast-mobile segments where the reorientation occurs on the timescale of dangling chains.

We shall consider in the following a log-Gauss distribution for the correlation time [35], i.e.,

Table 2
Averaged residual second moment $\langle \widetilde{M}_2 \rangle$, the center of gravity $\tau_{c,0}$, and width of decimal logarithm $\Delta\tau_c$ of unfilled and filled EPDM composites.

Samples	Filler content (phr)	Averaged values		Distribution of correlation time		
		$\langle \widetilde{M}_2 \rangle$ (10^6 rad^2/s^2)	$\langle \tau_c \rangle$ (μs)	$\langle \widetilde{M}_2 \rangle$ (10^6 rad^2/s^2)	τ_{c0} (μs)	$\Delta\tau_c$
Unfilled	0	2.45	230	1.76	341	0.24
N683	20	5.66	115	2.70	256	0.23
N683	40	3.44	181	2.25	294	0.23
N683	60	2.78	220	2.01	321	0.22
N683	70	2.19	280	1.76	369	0.21

*Fit errors were smaller than 5%.

$$f(\tau_c) = G_{\ln}(\tau_c) = \frac{1}{\Delta\tau_c\sqrt{2\pi}} \exp\left\{-\frac{\ln^2(\tau_c/\tau_{c,0})}{2\Delta\tau_c^2}\right\}, \quad (14)$$

where the Δ is the width of the Gaussian function on the logarithmic scale and the $\tau_{c,0}$ is the center of the logarithmic distribution. Finally, the Hahn-echo decay is given by,

$$\frac{S_{HE}(2\tau)}{S_{HE}(0)} = \frac{1}{\Delta\tau_c\sqrt{2\pi}} \int_0^\infty \exp\left\{-\frac{\ln^2(\tau_c/\tau_{c,0})}{2\Delta\tau_c^2}\right\} \times \exp\left[-\sqrt{\frac{3}{2}}\langle\tilde{M}_2\rangle\tau_c^2\left(e^{-2\tau/\tau_c} + 2\tau/\tau_c - 1\right)\right] d\tau_c. \quad (15)$$

A fit program based on the Levenberg–Marquardt algorithm was written in C++ to extract $\langle\tilde{M}_2\rangle$, the center of gravity $\tau_{c,0}$, and the width $\Delta\tau_c$ of the distribution. Such distribution of correlation times describes the polymer chain dynamics more realistically and produces a much better fit of experimental data as one can observe in Fig. 5b where the continuous line passes through all points. In this sense the merit function obtained from the fit with Eq. (15) of the Hahn-echo decay for the EPDM filled with 20 phr N683 filler was found to be $\chi^2 = 9.3 \times 10^{-5}$. The overall results are summarized in Table 2.

3.6. Distribution of the ^1H residual second moment

If the experimental data are fitted with a function that depends on a product of $\tilde{M}_2$, and τ_c, then the results are characterized by a high degree of uncertainty. This problem can be partially be solved by considering a new approximation of an averaged correlation time $\bar{\tau}_c$ to describe the segmental dynamics regardless of the filler type. For the value of $\bar{\tau}_c$ we have used the previous results of centers $\tau_{c,0}$ given in Table 2.

When the fast Laplace inversion algorithm [34] is applied to the experimental data to determine the distribution $f(\tilde{M}_2)$ of the residual second moment than the Hahn-echo decay has to be considered,

$$\frac{S_{HE}(2\tau)}{S_{HE}(0)} = \sum_{i=1}^{N} f(\tilde{M}_{2,i}) \exp\left[-\sqrt{\frac{3}{2}}\tilde{M}_{2,i}\bar{\tau}_c^2\left(e^{-2\tau/\tau_c} + 2\tau/\bar{\tau}_c - 1\right)\right] d[\log_{10}(\tilde{M}_2)]. \quad (16)$$

Due to the discrete nature of experimental data the integral from Eq. (8) is transformed into a Darboux sum over a number N of distributed points which can be chosen large enough to have a smooth distribution. The distribution of $\tilde{M}_2$ will be obtained on a logarithmic scale. While analyzing the data obtained from an algorithm based on the inverse Laplace transformation, which applies to an ill-conditioned problem, we have to be careful in the interpretation since artefacts like the *pearling effects*, can occur [36]. Often, these effects are related to bad choices of the distribution domain or the regularization parameter α [34,36]. This kind of a problem can be identified by instability of the distribution to changes in parameters of the algorithm. Although in this work the stability test was performed, a small degree of incertitude remains since the regularization parameter α was kept constant. The main reason was that the peak widths dependent on α and we would like to be able to compare all samples for which the experimental data were measured using the same processing conditions.

The normalized distributions of ^1H residual second moments $\tilde{M}_2$ are presented in Fig. 6 for the EPDM elastomers reinforced with N683 carbon-black fillers. The distributions were obtained by applying the inversion Laplace procedure using Eq. (16) where the average correlation time was taken to be $\bar{\tau}_c = 316$ μs. In order to be compared directly, all distributions are normalized; i.e., the integral area under the distribution is unity on the logarithmic scale. For comparison the distribution of unfilled EPDM rubber is presented in Fig. 6 together with the $\tilde{M}_2$ distributions of filled samples. The $\tilde{M}_2$ distributions of unfilled EPDM samples are characterized by two distinct peaks. The main peak is centered at $\tilde{M}_2 \sim 2.1 \times 10^6$ rad^2 s^{-2} but one can observe also a smaller peak at a lower value of $\tilde{M}_2$ that could be related to the more mobile segments.

The interaction between N683 carbon-black filler clusters and polymer chains, at low filler content values (20 phr), leads to the

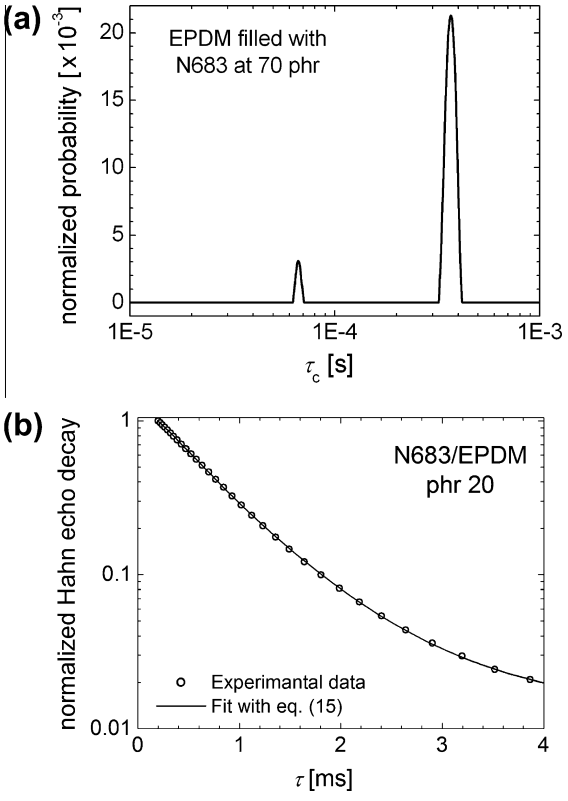

Fig. 5. (a) Normalized probability distribution of correlation times τ_c obtained by Laplace inversion of Eq. (13) for the averaged value of the residual second moment $\langle\tilde{M}_2\rangle = 1.7 \times 10^6$ rad^2 s^{-2}. The EPDM sample reinforced with 70 phr N683 carbon-black fillers was considered. (b) The best fit ($\chi^2 = 9.3 \times 10^{-5}$) of the Hahn-echo decay for 20 phr N683 fillers in EPDM with the exponential correlation function and a log-Gauss distribution of correlation time characterized by the center of gravity at $\tau_{c,0} = 256$ μs and the width on log scale of $\Delta\tau_c = 0.23$. The averaged residual second moment is $\langle\tilde{M}_2\rangle = 2.7 \times 10^6$ rad^2 s^{-2} .

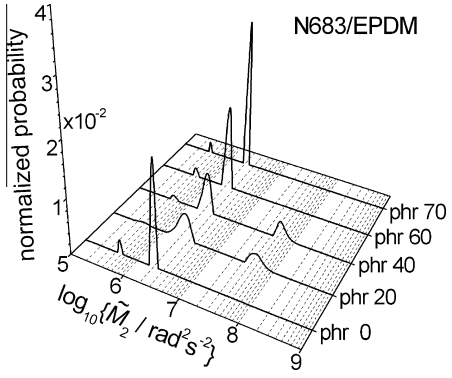

Fig. 6. Normalized probability distribution of the residual second moment $\tilde{M}_2$ for the EPDM samples filled with carbon-black filler N683 for 20, 40, 60 and 70 phr filler contents. The normalized probability distribution for unfilled EPDM is also shown.

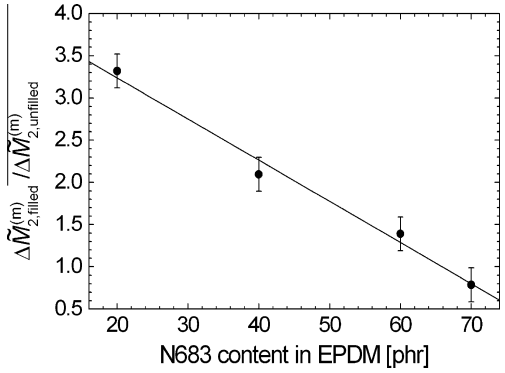

Fig. 7. The width at half height of filled N683/EPDM samples normalized to the same quantity of unfilled EPDM $\Delta\widetilde{M}^{(m)}_{2,filled}/\Delta\widetilde{M}^{(m)}_{2,unfilled}$ of the main peaks of mobile polymer segments from distributions of Fig. 6 shown as a function of filler content.

apparition of peaks from the interface chains and a broad mobile main peak. With the increase of the N683 content (40 phr), the peak located at high $\widetilde{M}_2$ value, which correspond to the interface chains, is shifted towards larger values. For larger N683 filler contents the strong filler–polymer chain interactions constrain the mobility of chain segments, therefore the interface peaks are no longer observed for 60 and 70 phr concentration.

The main mobile peak width at half height of filled samples normalized to the same quantity of unfilled sample $\Delta\widetilde{M}^{(m)}_{2,filled}/\Delta\widetilde{M}^{(m)}_{2,unfilled}$ function of filler content is shown in Fig. 7. The increase of filler clusters sizes leads to an increased filler surface to which the polymer chains can be confined, therefore the distribution of mobile polymer chain segments characterized by the residual second moment is reduced. A linear decay of the normalized peak width $\Delta\widetilde{M}^{(m)}_{2,filled}/\Delta\widetilde{M}^{(m)}_{2,unfilled}$ function of filler content was observed for N683/EPDM samples (Fig. 7).

4. Conclusions

The dynamic heterogeneities of polymer chains has been studied systematically for a series of EPDM elastomers with carbon-black N683 filler contents varying from 20 phr to 70 phr. Proton Hahn-echo decays were measured with an acquisition delay that plays the role of a dipolar filter and removes the signal contribution from the bound polymer chains. The Hahn-echo decay was considered which is weighted only by the fluctuating part of the polymer chains. An exponential correlation function was considered in the derivation of the functional form for the Hahn-echo decay. The power-law correlation function was found to be inadequate to describe the Hahn-echo decay of mobile EPDM segments for carbon-black filled samples in the investigated time domain.

The distributions of residual second moment $\widetilde{M}_2$ and the correlation time τ_c were included in functions that describe the Hahn-echo decays. Due to the mathematical complexity of the problem when distributions are used for both quantities two limiting cases were treated: (i) an average value of $\langle\widetilde{M}_2\rangle$ and a log-Gauss distribution for the correlation times; and (ii) an average value for $\bar{\tau}_c$ and a distribution of $\widetilde{M}_2$ values. In the second case a fast inverse Laplace transformation was used to obtain the $\widetilde{M}_2$ distributions for all samples.

The effects of fillers on the heterogeneity of the segmental dynamics are observed by: (i) the large distribution of mobile peaks and (ii) the apparition at low filler content of a third peak in addition to those two of unfilled EPDM. The peaks are located at higher $\widetilde{M}_2$ values indicating a reduced mobility which is associated with interface segments between mobile chain segments and bound rubber. For the EPDM reinforced with N683 carbon-black the mechanism of chain adsorption by an increased surface of filler clusters seems to be based on the adsorption of mobile segments during the increase of filler content which are transformed in bound rubber. This assumption is supported by the observed decay of the peaks distribution that corresponds to the mobile polymer segment while increasing the filler content.

Acknowledgments

This project was partially supported by a grant of the Romanian Ministry of Education and Research under Project PN II-ID 1102/2007. B.B. gratefully acknowledges support by Deutsche Forschungsgemeinschaft with Project BL 231/37-1.

References

[1] T.A. Vilgis, G. Heinrich, M. Klüppel, Reinforcement of Polymer Nano-Composites, Theory, Experiments and Applications, Cambridge University Press, 2009.
[2] G. Heinrich, M. Klüppel, T.A. Vilgis, Reinforcement Theories in Physical Properties of Polymers Handbook, second ed., Springer, Heidelberg, 2007.
[3] T.A. Vilgis, Time scales in the reinforcement of elastomers, Polymer 12 (2005) 4223.
[4] J.L. Leblanc, Filled Polymers, Science and Industrial Applications, CRC Press Taylor & Francis Group, Boca Raton, London, New York, 2009.
[5] J.L. Leblanc, Rubber–filler interactions and rheological properties in filled compounds, J. Prog. Polym. Sci. 27 (2002) 627.
[6] V.J. McBrierty, J.C. Kenny, Structural investigations of carbon black-filled elastomers using NMR and ESR, Kaut. Gummi Kunstst. 47 (1994) 342–348.
[7] V.M. Litvinov, P.A.M. Steeman, EPDM-carbon black interactions and the reinforcement mechanisms, as studied by low-resolution ^{1}H NMR, Macromolecules 32 (1999) 8476–8490.
[8] Ramona A. Orza, Pieter C.M.M. Magusin, Victor M. Litvinov, Martin van Duin, M.A.J. Michels, Solid-state ^{1}H NMR study on chemical cross-links, chain entanglements, and network heterogeneity in peroxide-cured EPDM rubbers, Macromolecules 40 (2007) 8999–9008.
[9] Z. Zhu, T. Thompson, S.Q. Wang, E.D. von Meerwall, A. Halasa, Investigating linear and nonlinear viscoelastic behavior using model silica-particle-filled polybutadiene, Macromolecules 38 (2005) 8816.
[10] G.I. Sandakov, L.P. Smirnov, A.I. Sosikov, K.T. Summanen, N.N. Volkova, NMR analysis of distribution of chain lengths between crosslinks of polymer networks, J. Polym. Sci. Part B: Polym. Phys. 32 (1994) 1585–1592.
[11] D. Moldovan, R. Fechete, D.E. Demco, E. Culea, B. Blümich, V. Herrmann, M. Heinz, Macromol. Chem. Phys. 211 (2010) 1579.
[12] K. Hailu, R. Fechete, D.E. Demco, B. Blümich, Segmental anisotropy in strained elastomers detected with a portable NMR scanner, Solid State Nucl. Magn. Reson. 22 (2002) 327–343.
[13] R.I. Chelcea, R. Fechete, E. Culea, D.E. Demco, B. Blümich, Distributions of transverse relaxation times for soft-solids measured in strongly inhomogeneous magnetic fields, J. Magn. Reson. 196 (2009) 178–190.
[14] A. Wiesmath, C. Filip, D.E. Demco, B. Blümich, NMR of multipolar spin states excited in strongly inhomogeneous magnetic fields, J. Magn. Reson. 154 (2002) 60–72.
[15] R. Kimmich, NMR: Tomography, Diffusiometry, Relaxometry, Springer-Verlag, Berlin, Heidelberg, New York, 1997.
[16] E. Fischer, F. Grinberg, R. Kimmich, Characterization of polymer networks using the dipolar correlation effect on the stimulated echo and field-cycling nuclear magnetic resonance relaxometry, J. Chem. Phys. 109 (1998) 846–854.
[17] R.C. Ball, P.T. Callaghan, E.T. Samulski, A simplified approach to the interpretation of nuclear spin correlations in entangled polymeric liquids, J. Chem. Phys. 106 (1997) 17.
[18] D.A. Vega, M.A. Villar, E.M. Vallés, C.A. Steren, G.A. Monti, Comparison of mean-field theory and ^{1}H NMR transversal relaxation of poly(dimethylsiloxane) networks, Macromolecules 34 (2001) 283–288.
[19] J.-P. Cohen-Addad, NMR and fractal properties of polymeric liquids and gels, in: J.W. Emsley, J. Feeney, L.H. Sutcliffe (Eds.), Progress in NMR Spectroscopy, vol. 25, Pergamon Press, Oxford, 1993, pp. 1–316.
[20] P. Sotta, C. Fülber, D.E. Demco, B. Blümich, H.W. Spiess, Effect of residual dipolar interactions on the NMR relaxation in cross-linked elastomers, Macromolecules 29 (1996) 6222–6230.
[21] M.A. Voda, D.E. Demco, J. Perlo, R.A. Orza, B. Blümich, Multispin moments edited by multiple-quantum NMR: application to elastomers, J. Magn. Reson. 172 (2005) 98–109.
[22] E. Gjersing, S. Chinn, J.R. Giuliani, J. Herberg, R.S. Maxwell, E. Eastwood, D. Bowen, T. Stephens, Investigation of network heterogeneities in filled, trimodal, highly functional PDMS networks by ^{1}H multiple quantum NMR, Macromolecules 40 (2007) 4953–4962.
[23] J.P. Lewicki, R.S. Maxwell, M. Patel, J.L. Herberg, A.C. Swain, J.J. Liggat, R.A. Pethrick, Effect of meta-carborane on segmental dynamics in a bimodal poly(dimethylsiloxane) network, Macromolecules 41 (2008) 9179–9186.

[24] J.L. Valentín, I. Mora-Barrantes, J. Carretero-González, M.A. López-Manchado, P. Sotta, D.R. Long, K. Saalwächter, Novel experimental approach to evaluate filler–elastomer interactions, Macromolecules 43 (2010) 334–346.
[25] Kay Saalwächter, Proton multiple-quantum NMR for the study of chain dynamics and structural constraints in polymeric soft materials, Prog. NMR Spectrosc. 51 (2007) 1–35.
[26] R. Fechete, D.E. Demco, B. Blümich, Enhanced sensitivity to residual dipolar couplings of elastomers by high-order multiple-quantum NMR, J. Magn. Reson. 169 (2004) 19–26.
[27] P.T. Callaghan, E.T. Samulski, The molecular weight dependence of nuclear spin correlations in entangled polymeric liquids, Macromolecules 31 (1998) 3693–3705.
[28] P.T. Callaghan, E.T. Samulski, Molecular ordering and the direct measurement of weak proton–proton dipolar interactions in a rubber network, Macromolecules 30 (1997) 113–122.
[29] R. Fechete, D.E. Demco, B. Blümich, Chain orientation and slow dynamics in elastomers by mixed magic-Hahn echo decays, J. Chem. Phys. 118 (2003) 2411.
[30] D.E. Demco, R. Fechete, B. Blümich, Residual dipolar couplings of soft solids by accordion magic sandwich, Chem. Phys. Lett. 375 (2003) 406–412.
[31] F.V. Chávez, K. Saalwächter, NMR observation of entangled polymer dynamics: tube model predictions and constraint release, Phys. Pew. Lett. 104 (2010) 198305.
[32] Y.Q. Song, L. Venkataramanan, M.D. Hürlimann, M. Flaum, P. Frulla, C. Straley, T_1–T_2 correlation spectra obtained using a fast two-dimensional Laplace inversion, J. Magn. Reson. 154 (2002) 261–268.
[33] M.D. Hürlimann, M. Flaum, L. Venkataramanan, C. Flaum, R. Freedman, G.J. Hirasaki, Diffusion-relaxation distribution functions of sedimentary rocks in different saturation states, Magn. Reson. Imaging 21 (2003) 305–310.
[34] L. Venkataramanan, Y.Q. Song, M.D. Hürlimann, Solving fredholm integrals of the first kind with tensor product structure in 2 and 2.5 dimensions, IEEE Trans. Signal Process. 50 (2002) 1017–1026.
[35] K. Schmidt-Rohr, H.W. Spiess, Multidimensional Solid-State NMR and Polymers, Academic Press Limited, London NY, 1999.
[36] K.E. Washburn, P.T. Callaghan, Tracking pore to pore exchange using relaxation exchange spectroscopy, Phys. Rev. Lett. 97 (2006) 175502.